High precision predictions for exclusive VH production at the LHC

Ye Li[1, *] and Xiaohui Liu[2, 3, †]

^{1}SLAC National Accelerator Laboratory,
Stanford University, Stanford, CA 94309
^{2}High Energy Division, Argonne National Laboratory, Argonne, IL 60439
^{3}Department of Physics and Astronomy,
Northwestern University, Evanston, IL 60208

Abstract

We present a resummation-improved prediction for $pp \to VH + 0$ jets at the Large Hadron Collider. We focus on highly-boosted final states in the presence of jet veto to suppress the $t\bar{t}$ background. In this case, conventional fixed-order calculations are plagued by the existence of large Sudakov logarithms $\alpha_s^n \log^m(p_T^{veto}/Q)$ for $Q \sim m_V + m_H$ which lead to unreliable predictions as well as large theoretical uncertainties, and thus limit the accuracy when comparing experimental measurements to the Standard Model. In this work, we show that the resummation of Sudakov logarithms beyond the next-to-next-to-leading-log accuracy, combined with the next-to-next-to-leading order calculation, reduces the scale uncertainty and stabilizes the perturbative expansion in the region where the vector bosons carry large transverse momentum. Our result improves the precision with which Higgs properties can be determined from LHC measurements using boosted Higgs techniques.

*Electronic address: yli@slac.stanford.edu
†Electronic address: xiaohuiliu@anl.gov

I. INTRODUCTION

With the confirmation of the existence of a Higgs particle by both the CMS and ATLAS collaborations [1, 2] at the Large Hadron Collider (LHC), one of the main objectives of the LHC is to test as many of its properties as possible. The experimental discovery channel is based on its bosonic decay only, and it becomes crucial to probe its couplings to fermions directly to verify whether they agree with Standard Model predictions. However, the standard Higgs production channel of gluon fusion suffers from large QCD backgrounds in its fermion decay modes. The so-called Higgsstrahlung process provides another important way of Higgs measurement at hadron colliders, where the Higgs is produced in association with either a W or Z vector boson (we will refer to them generally as V). It was the main search channel for a light Higgs at the Tevatron. At the LHC, the large background from the semi-leptonic decay of the $t\bar{t}$ process obscures the Higgs signal and leads to a poor signal to background ratio. However, recent studies [3] have shown that with techniques such as jet substructure and large transverse momentum cuts on the Higgs and the vector boson, the Higgsstrahlung process offers a viable alternative to study the fermion decay channel [4–7] as well as possible invisible decays of the Higgs [8, 9]. To further suppress the unwanted backgrounds, both CMS and ATLAS adopt a jet veto procedure allowing no extra jets with p_T greater than $p_T^{veto} \sim 25\text{GeV}$.

Though effective in the experimental analysis, on the theory side, imposing a jet veto with p_T^{veto} much less than the center of mass energy at which the hard processes take place leads to large Sudakov logarithms that can destabilize the perturbative series in conventional perturbative QCD calculations. It has been shown that the impact of QCD corrections is sizable for events with W and H boosted at large p_T in the presence of jet veto[1] in Ref. [13], where the fully exclusive cross section for WH production up to next-to-next-to-leading order (NNLO) in QCD was studied. The jet veto reverses the sign of the higher-order QCD correction compared to the inclusive case, and reduces the total cross section. Recently there have been works on the transverse-momentum resummation of $V + H$ [14] and on the jet veto resummation [15] for the Higgsstrahlung process. Neither study addressed the impact of the jet veto as a function of the transverse momentum of V or H, which is required to understand the QCD corrections in the boosted phase-space region.

In this manuscript, we present the fully exclusive cross section for VH production at NNLO in QCD matched with the resummation of jet veto logarithms at the partial next-to-next-to-leading-log prime (NNLL_p') accuracy and study the relevant theoretical uncertainty.

---

[1] The imposed jet veto makes the lower p_T cut on the vector boson equivalent to that on the Higgs in the boosted region.

We follow the counting of logarithmic accuracy according to Ref. [25], and the subscript p stands for "partial", indicating that we have not included the non-logarithmically enhanced contributions at $\mathcal{O}(\alpha_s^2)$, the effect of which is found to be small. In the small-jet-radius limit, our calculation is expected to be comparable with the NNLL′ accuracy. Compared to Ref. [15], we have achieved higher accuracy in both the resummation and the fixed order calculation. In addition, we follow the experimental analysis more closely by studying the transverse momentum dependence of the cross section and focusing on the impact of the resummation in the boosted region of V and H.

The resummation of jet veto logarithms to NNLL′$_p$ relies on recent developments in the soft collinear effective theory (SCET) [18–22], which has been applied successfully to the $H + 0j$ production [23–25]. Using the effective theory, the $H + 1j$ case was studied in Ref. [26] and Ref. [27] for $p_T^J \sim m_H$ and was extended to the challenging low jet p_T region in Ref. [28]. A complete framework for the combination of resummed results for production processes in different exclusive jet bins was also presented in Ref. [28]. A systematic study on the jet veto clustering effects up to $\mathcal{O}(\alpha_s^3)$ in the small-jet-radius limit was carried out in Ref. [29].

The NNLO QCD correction is obtained by modifying the numerical code FEWZ [30–32], originally used to calculate the DY process. The heavy-quark induced process is not included. Higgs production in association with a vector boson is dominated by DY like processes up to next-to-leading order (NLO) in QCD. At NNLO, there are small contribution from the process where the Higgs is produced via heavy quark loop induced by gluon pairs. Its contribution is found to be around 1%(1%) for WH and 5%(9%) for ZH inclusive cross section for an 8 TeV (14 TeV) LHC [33]. This is expected to be further suppressed in the region where the vector boson and Higgs carry large transverse momentum[2]. Furthermore, the decay of the vector boson into lepton final states is available as a result of the nature of the original FEWZ. The modification is validated via a series of numerical checks against MCFM [34] for differential observables at NLO, Sherpa [35] for VH plus 1 or 2 jet(s) exclusive results, as well as VH@NNLO [33] for inclusive cross sections. In this study, we integrate over the lepton phase space inclusively for better numerical stability. We found that the scale uncertainty gets reduced and the convergence of the perturbative series is improved dramatically after resumming the jet veto logarithms. The results of our analysis should stay largely unaffected in the presence of standard experimental acceptance cuts due to the absence of new phase space singularities at the given perturbative order.

Our manuscript is organized as follows. In section II, we briefly review the theoretical

---

[2] for the ZH process, this subleading process actually is enhanced below the top pair threshold, but here we will only focus on the resummation on its DY like contribution for the purpose of this manuscript.

set-up in the resummation of jet veto logarithms. In section III, we present the numerical consequence of the resummation for both ZH and WH production at the LHC. We adopt cuts similar to the current experimental analyses and concentrate on the highly-boosted region. Finally, we conclude in Section IV. All necessary technical details are given in the Appendix.

II. REVIEW OF THE THEORETICAL FORMALISM

In this section, we briefly review the theoretical framework for understanding jet vetoed cross sections at hadron colliders. The formalism has been established in a series of works for both 0 jet and exclusive 1 jet based on either the QCD coherence argument [16, 17] or the effective theory analysis [23–28]. Our approach relies on the recently developed works in SCET [18–22]. Here we will only highlight the formulae used in our calculation and we refer the readers to Refs. [23–27] for a detailed discussion and derivation of the factorization theorem for jet vetoed cross sections and to Refs. [36, 37] for short reviews. We group all the necessary ingredients for NNLL'_p resummation in the Appendix.

A. factorization, resummation and matching

When p_T^{veto} is much less than the energy scale Q which characterizes the production process, the cross section can be approximated by a factorized piece with an additional term,

$$\frac{\mathrm{d}^2\sigma}{\mathrm{d}Q^2\mathrm{d}Y} = \frac{\mathrm{d}\hat{\sigma}_B}{\mathrm{d}Q^2} H(Q^2,\mu) \, B\left(x_a, p_T^{veto}, R, \mu, \nu\right) \, B\left(x_b, p_T^{veto}, R, \mu, \nu\right) \, S\left(p_T^{veto}, R, \mu, \nu\right) + \sigma_0^{\mathrm{Rsub}},$$

(1)

up to contributions suppressed by p_T^{veto}/Q, where R is the jet size parameter for the clustering algorithm. Here $\mathrm{d}\hat{\sigma}_B$ is the Born level partonic cross section initiating the relevant process. For instance for ZH production the Born level cross section comes from the tree level process $q\bar{q} \to Z^* \to ZH \to l^+l^-H$ and $q\bar{q} \to WH \to \nu l H$. Here Q^2 and Y are the invariant mass square and rapidity of the entire final state, respectively. The Bjorken scale parameter x is given by

$$x_{a,b} = \frac{Q}{E_{cm}}e^{\pm Y} \in (0,1),$$

(2)

with E_{cm} denoting the machine center of mass energy. Here H, B and S are the hard function, beam function for describing the collinear radiations in the forward region and soft

4

function for the radiations with low energies. Their field theoretic definition can be found in Ref [23]. Their explicit form up to $\mathcal{O}(\alpha_s^2)$ is given in the Appendix.

Due to the homogenous expansion in SCET_{II} where the soft and the collinear modes share the same scaling in their virtualities, other than the normal divergence regulated by the renormalization scale μ in the dimensional regularization, there exists additional rapidity divergences which are regulated by a new fictitious scale ν in both the beam and soft functions [38, 39]. The regularization scheme gives rise to a new renormalization group equation in SCET, which eventually allows us to sum up the full set of large logarithms of the form $\log(p_T^{veto}/Q)$ to all orders, by evolving each function in Eq. (1) from its natural scales (μ_i, ν_i) to the common scales (μ, ν). The scales (μ_i, ν_i) are estimated by demanding that in each function the perturbative series behaves properly. Therefore, we have

$$\mu_H \sim -iQ, \quad \mu_B \sim \mu_S \sim p_T^{veto},$$
$$\nu_B \sim Q, \qquad \nu_s \sim p_T^{veto}. \tag{3}$$

Here choosing the imaginary scale $\mu_H \sim -iQ$ allows us to sum up a tower of large π^2 terms for time-like processes [40].

Eq. (1) also contains a non-factorizable correction term,

$$\sigma_0^{\text{Rsub}} \propto \left(\frac{\alpha_s C_F}{4\pi}\right)^2 \left(\frac{16\pi^2}{3}R^2 - 4R^4\right) \log \frac{p_T^{veto}}{Q}, \tag{4}$$

which contributes at the NNLL'_p level especially when $R \sim 1$. As argued in Refs [16, 17], the overall coefficient determines the complete logarithmic series coming from this term. Therefore, we follow the procedure in Ref. [25] to include this piece in the resummed cross section at NNLL'_p by multiplying it with the total evolution factor.

The SCET cross section Eq. (1) only gives the exact result when $p_T^{veto}/Q \to 0$. When away from zero, the missing power-suppressed term may have a sizable effect on the cross section. In order to recover its contribution, we have to match the SCET calculation onto the fixed-order QCD cross section. Here we adopt the most straightforward matching scheme, in which we subtract the most singular terms in p_T^{veto}/Q predicted by SCET up to two loops, from the NNLO QCD cross section, and replace that by the NNLL'_p along with π^2 resummed one (see, section III). The final result for the resummation-improved cross section is

$$\sigma_{\text{NNLL}'_p+\text{NNLO}} = \sigma_{\text{NNLO}} - \sigma_{\text{NNLL}'_p}^{\text{sing.}} + \sigma_{\text{NNLL}'_p}^{\text{resum}}. \tag{5}$$

Here σ_{NNLO} is the NNLO cross section obtained based on a modification of the FEWZ code, detailed in Appendix A. The SCET expanded cross section $\sigma_{\text{NNLL}'_p}^{\text{sing.}}$ contains all the $\mathcal{O}(\alpha_s^2)$ order singular contributions to σ_{NNLO}, and $\sigma_{\text{NNLL}'_p}^{\text{resum}}$ denotes the cross section for with $\text{NNLL}'_p + \pi^2$ resummation. All the building blocks needed for $\sigma_{\text{NNLL}'_p}^{\text{sing.}}$ and $\sigma_{\text{NNLL}'_p}^{\text{resum}}$ can be found in the Appendix.

B. $\log(R)$ dependent contributions

For a complete NNLL$'$ p_T^{veto}-resummation, all the matrix elements should be computed up to $\mathcal{O}(\alpha_s^2)$ (see for instance, Ref. [25]). Starting from the α_s^2 order, clustering effects will give rise to $\log(R)$ dependent contributions, which, for small jet radius, dominate over the other non-$\log(p_T^{veto}/\mu)$ enhanced terms of the two loop matrix elements. The $\log(R)$ corrections at α_s^2 appearing in both the soft and beam functions comes from the clustering of two correlated radiations coming from a single collinear splitting of distance roughly R into two different jets. They can therefore be extracted from the strongly ordered collinear behavior of QCD, given by

$$\Delta|\mathcal{M}|^2_{jk,\text{NNLO}} = \int [\mathrm{d}k]\,\mathrm{d}x\,|\mathcal{M}|^2_{i,\text{NLO}}(k_T, z, \mu, \nu, \epsilon, \eta) \int \frac{\mathrm{d}q_\perp^2}{q_\perp^2} \frac{\alpha_s}{2\pi} P_{jk\leftarrow i}(x)\,\Theta(\Delta R - R)\Delta\hat{\mathcal{F}}_{veto}\,,$$

(6)

where, $|\mathcal{M}_{i,\text{NLO}}|^2$ is the one loop soft or beam function with properly regularizing the divergence in the effective theory and $P_{jk\leftarrow i}(x)$ is the one loop splitting function. The transverse momentum $q_\perp$ is with respect to the mother particle i before splitting and $\Delta\hat{\mathcal{F}}_{veto}$ is the phase space measure which accounts for the jet algorithm. We note that an additional symmetry factor should be included when evaluating $g \to gg$ or $q \to qg$ with the gluon or the quark further splitting, respectively, in the beam function.

Using the fact that in the small R limit,

$$\Delta R^2 \approx \frac{q_\perp^2}{k_T^2 z^2(1-z)^2}\,,$$

(7)

and writing out explicitly the measure $\Delta\hat{\mathcal{F}}_{veto}$, we get

$$\begin{aligned}
\Delta|\mathcal{M}|^2_{jk,\text{NNLO}} &= \frac{\alpha_s}{2\pi}\int [\mathrm{d}k]\,\mathrm{d}x\,|\mathcal{M}|^2_{i,\text{NLO}}(k_T, z, \mu, \nu, \epsilon, \eta) \\
&\times \int_R^{\sim 1} \frac{\mathrm{d}\Delta R^2}{\Delta R^2} P_{jk\leftarrow i}(x) \left[\Theta\left(p_T^{veto} - \max(x, 1-x)k_T\right) - \Theta\left(p_T^{veto} - k_T\right)\right]\,.
\end{aligned}$$

(8)

Using the equation above, all the α_s^2 order $\log(R)$ terms, either in the anomalous dimensions or in the matrix elements, can be calculated in a straightforward way. For our purposes, we have the following p_T^{veto} independent $\log(R)$ terms in the beam function:

$$\begin{aligned}
I^{(2)}_{q_i q_i,\log R} &= \frac{2}{9}C_F\left(\left(-12\pi^2 + 131 - 132\log(2)\right)C_A + (24\log(2) - 23)n_f T_F\right)\log(R^2)\,p^{(0)}_{q_i q_i}(z)\,, \\
I^{(2)}_{q_i g,\log R} &= 4C_F T_F\left(-\frac{\pi^2}{3} + 3 - 3\log(2)\right)\log(R^2)p^{(0)}_{q_i,g}(z)\,,
\end{aligned}$$

(9)

where $p_{ij}^{(0)}(z)$ is the splitting function which can be found in the appendix.

We note that other than the $\log(R)$ contributions, we also need the non-$\log(R)$ enhanced p_T^{veto} independent terms at $\mathcal{O}(\alpha_s^2)$ for claiming NNLL$'$ accuracy. The analytic formula for the full two loop soft function including these contributions is known [25], and is listed in the appendix. For the beam function, those terms can be obtained easily by comparing the fixed two loop SCET expansion with the full NNLO QCD calculation. We found that for $pp \to VH$, these contributions are numerically negligible for both large and small R, therefore in this work we do not include their contributions and denote our accuracy as NNLL$'_p$.

III. NUMERICAL RESULTS

We start the section by demonstrating the validity of the SCET factorization theorem numerically. Later on, we will introduce our scale choices and our strategy for the theoretical uncertainty estimation.

In Fig. 1, we show the comparison of the cross section $\sigma(p_T^{veto})$ with a jet veto between the QCD prediction and the SCET calculation up to NNLO in α_s. The results are given as a function of p_T^{veto} for both ZH and WH production at the LHC with $14\,\text{TeV}$ machine energy (LHC14). The jets are constructed using anti-k_T jet algorithm with $R = 1.2$. For small p_T^{veto}, the two calculations differ by a non-logarithmically enhanced constant piece (independent of p_T^{veto}) at $\mathcal{O}(\alpha_s^2)$, in addition to p_T^{veto}/Q power suppressed terms. The numerical results presented in Fig. 1 shows almost no differences between them for small p_T^{veto}. The differences are found to be around or less than per mil level.
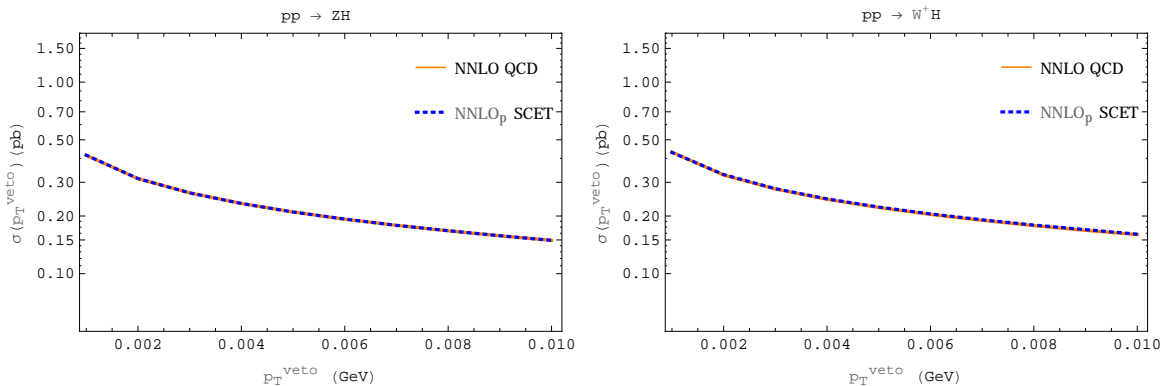

FIG. 1: We compare the NNLO QCD (red solid) cross section with the expanded NNLL to $\mathcal{O}\left(\alpha_s^2\right)$ from SCET prediction (blue dotted) for both ZH with $p_Z^T > 100\,\text{GeV}$ (left panel) and W^+H with $p_W^T > 180\,\text{GeV}$ production (right panel) at LHC14. We focus on the small values of p_T^{veto}.

As p_T^{veto} increases, the size of the power-suppressed term starts to grow and becomes important when p_T^{veto} is comparable with Q. The power suppressed term is properly included in our prediction via the matching procedure, Eq. (5), described in the previous section.

The growth of the power suppressed contribution leads to the idea of profile scales [25, 27] that smoothly turn off resummation and merge with the fixed-order predictions in the high p_T^{veto} region where the effective theory breaks down and the power suppressed terms dominate. However, in our present analysis, we focus a fixed p_T^{veto} of 25GeV and study boosted VH production. We expect that for such a small p_T^{veto}, the singular contributions dominate and must be resummed. Therefore instead of using profile scales, we parametrize the scales using their canonical values in SCET:

$$
\begin{aligned}
\mu &= m_V + m_H \,, \\
\mu_H &= -iQ = -i\sqrt{x_a x_b} E_{\text{com}}, \quad \mu_B = \mu_S = p_T^{veto} \,, \\
\nu_B &= Q, \qquad \nu_S = p_T^{veto} \,.
\end{aligned}
\tag{10}
$$

as our central scale choice. The imaginary hard scale choice μ_H allows a better convergent perturbative series in evaluating the hard function and a resummation of a towers of π^2 terms.

We default to

$$
\mu_R = \mu_F = \mu = m_V + m_H \,,
\tag{11}
$$

as the central scale for the fixed order calculation. We vary the scales up and down by a factor of two to estimate the scale uncertainty. For the fixed order results, we use the "Stewart-Tackmann-prescription" for the error estimation [42]:

$$
\Delta_{0j}^2 = \Delta_{\text{tot.}}^2 + \Delta_{>1j}^2 \,,
\tag{12}
$$

where $\Delta_{\text{tot.}}$ and $\Delta_{>1j}$ are the uncertainties for total and $1j$ inclusive cross sections, respectively, obtained by varying the scale up and down by a factor two. For the resummation improved predictions, we use

$$
\Delta_{0j}^2 = \Delta_{\text{coll.}}^2 + \Delta_{\text{resum}}^2 \,,
\tag{13}
$$

where $\Delta_{\text{coll.}}$ is computed by varying all the scales in the effective theory collectively. For Δ_{resum}, we vary each scale μ_i and ν_i independently and take the envelope of all the variations.

We now turn to discuss the main results of this work. In presenting our numerical results, we use the (N)NLO MSTW2008 PDF set [41] for (N)NLO and (N)NLL + (N)NLO results and set the value and running of the strong coupling constant α_s accordingly. We use $n_f = 5$

8

for the active number of quark flavors, and choose the G_μ scheme as the electroweak input parameters throughout our analysis. We will only discuss ZH and W^+H productions at LHC14 in this manuscript. Jets are formed with anti-k_T jet algorithm[3] with $R = 1.2$ [3] and are vetoed if they have transverse momentum greater than $p_T^{veto} = 25$ GeV.

We first study the stability of the perturbative predictions with and without the improvement from the jet veto resummation. Fig. 2 illustrates the impact of the resummation on the convergence of the ZH perturbative cross section predictions at LHC14. Here we plot the cross section as a function of the lower transverse momentum cut of the Z boson $p_{T,\min}^Z$. It is clear that the resummation of the jet veto logarithms (right panel) accelerates the convergence of the perturbative series compared to the pure fixed-order ones (left panel), as the $p_{T,\min}^Z$ curve from the NLL$'$ + NLO prediction almost overlaps with the NNLL$'_p$ + NNLO one, while the NLO prediction is off by a visible amount with respect to the NNLO result.

The same trends can be observed for the predictions of the W^+H production at LHC14 which are depicted in fig. 3. The convergence of the perturbative expansion is greatly improved after the resummation.
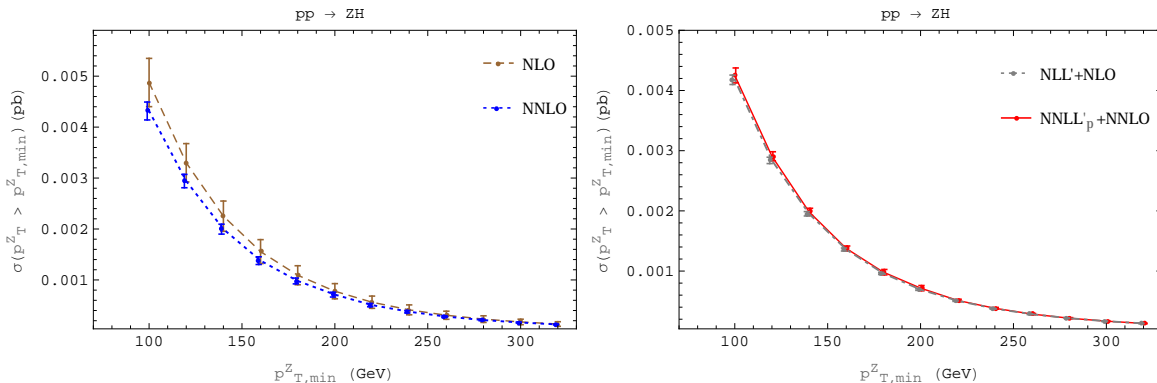

FIG. 2: The NLO (brown dashed) and NNLO (blue dotted) predictions for ZH production at LHC14 (left panel) along with the resummation improved NLL$'$ + NLO (gray dot-dashed) and NNLL$'_p$ + NNLO (red solid) results (right panel) are showed, as a comparison of the convergence of the perturbative series with and without the jet veto log resummation.

In both fig. 2 and fig. 3, the error bands reflect the scale uncertainties estimated using the prescriptions sketched previously in Eq. (12) and Eq. (13) for the pure fixed-order and the resummation improved predictions, respectively. Although the resummed predictions usually have more conservative handles over the perturbative uncertainties due to variation

---

[3] Here anti-k_T is selected for illustrative purposes only. There is no theoretical difficulty for us to switch to other k_T type jet algorithms, for instance Cambridge/Aachen, and the conclusions of this work will not be affected.

of multiple scales in the resummed cross section, we still observe sizable reductions in the theoretical errors after invoking the resummation.
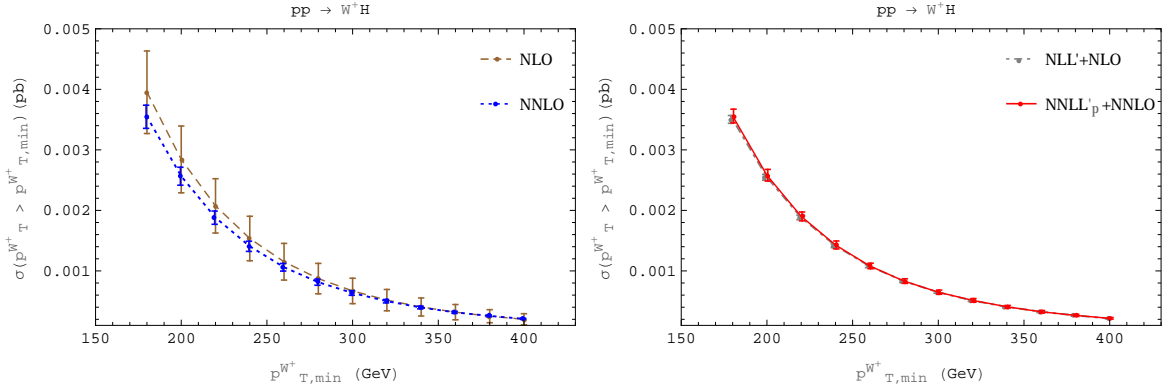

FIG. 3: Similar plots as fig. 2 for the convergence study on W^+H production at LHC14. The error bars denote the estimated theoretical scale uncertainties.

To see the reduction more clearly, we plot the NNLO and $NNLL'_p + NNLO$ predictions together in fig. 4 for both ZH and W^+H productions. The pure fixed-order and the resummed calculations yield central values close to each other, yet the resummed cross section comes along with a reduced scale dependence. For the experimentally interesting region ($p_{T,\min}^{Z,W} > 100, 180\,\text{GeV}$), the scale dependence drops from $\pm 5(6)\%$ to $\pm 3(4)\%$ for ZH (W^+H) production at LHC14, *i.e.* the theoretical error band shrinks by around 30%, and the veto efficiency for ZH and W^+H processes are roughly 47% and 41% respectively.
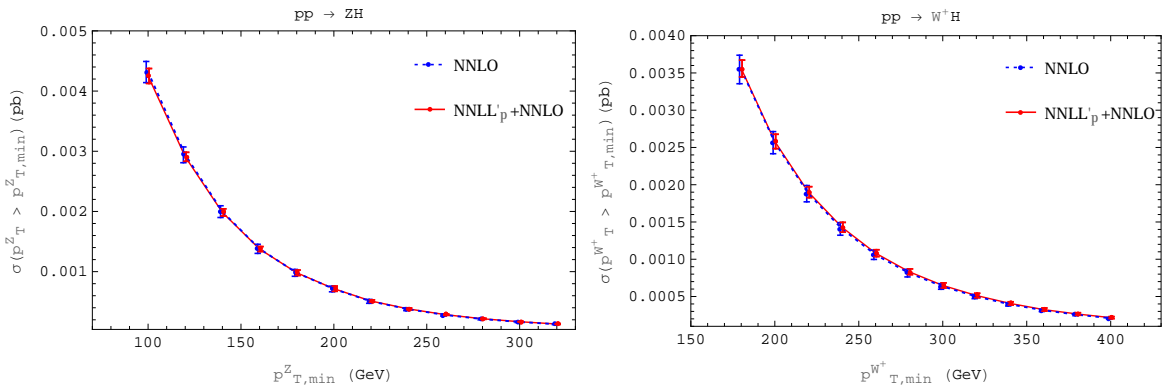

FIG. 4: The comparison between the NNLO cross sections with (red solid) and without (blue dotted) the $NNLL'_p + \pi^2$ resummation for both ZH (left panel) and W^+H production at LHC14. The error bars reflect the scale uncertainties.

10

IV. CONCLUSIONS

Recently, significant effort has been devoted to improved understanding of the Higgs cross section at the LHC, either using conventional NNLO calculations [43] or by utilizing resummation techniques [16, 17, 23–28]. In this work, we investigated the VH associated production process at the LHC. On the experimental side, a jet veto procedure demanding no jets with transverse momentum larger than p_T^{veto} is used by both CMS and ATLAS to suppress the backgrounds in the boosted Higgs analysis. However, theoretically the small value of $p_T^{veto} \ll m_V + m_H$ often destabilizes the perturbative expansion due to the existence of large logarithmic structure in the series. This makes the perturbative prediction unreliable and results in large theoretical uncertainties on the cross section as the p_T of the vector boson/Higgs increases. For VH production, when the transverse momentum p_V^T of the vector boson is required to be larger than $100 \sim 200\,\mathrm{GeV}$, the perturbative predictions suffer from roughly $\pm 6\%$ errors for LHC14 even at the NNLO. The limited power of the theoretical predictions restricts the accuracy that experimentalists can achieve. Also the large K factors in the presence of jet veto when one goes from LO, NLO to NNLO leads to the concern that the missing higher orders corrections may still be large and have sizable contributions to the cross section.

Here we improved the theoretical predictions through the resummation the jet veto logarithms and a series of π^2 terms up to NNLL'_p accuracy within the SCET framework. We further matched the resummed result onto the NNLO calculation to provide the full resummation improved cross section for VH production at hadron colliders. The improved results reduce the theoretical uncertainties. In the highly boosted regime, the scale uncertainty drops from $\pm 6\%$ to $\pm 4\%$ or below from NNLO to $\mathrm{NNLL}'_p + \mathrm{NNLO}$ for LHC14. Meanwhile resumming the jet veto logarithms greatly improves the convergence of the perturbative series in the region of interest experimentally. It can be seen from the fact that the central value remains virtually unchanged when one moves to higher orders in perturbative calculations, proving the reliability of the theoretical predictions. After resummation, the jet veto efficiency is found to be 47% and 41% for ZH and $W^+ H$, respectively.

In this manuscript, we highlight the general features of the resummation improved predictions for VH associated production, and show the power of resummation in reducing scale uncertainties and providing reliable central values. For illustration purpose here, we have chosen simplified cuts from the current experimental analysis without loss of generality. The results can be extrapolated for experimental use. In the future, extensive numerical studies on VH production with more practical cuts will be pursued in an upcoming paper, based on the scheme in this work.

Acknowledgments

Appendix A: modification of FEWZ

Here we give a brief introduction of the master formula we use to modify FEWZ for the Higgsstrahlung process. The squared matrix element of the DY process in FEWZ can be schematically written as,

$$\overline{|\mathcal{M}_V|^2} \sim Q_{\mu\nu} L^{\mu\nu}, \tag{A1}$$

where $Q_{\mu\nu}$ is the square of the quark current and includes all QCD corrections, and $L^{\mu\nu}$ is the square of the lepton current. As long as no observables related to asymmetry in the lepton phase space, we can neglect the axial part of the current, hence

$$L^{\mu\nu} \sim -g^{\mu\nu} l_1 \cdot l_2 + l_1^\mu\, l_2^\nu + l_1^\nu\, l_2^\mu. \tag{A2}$$

When integrated over the lepton phase space inclusively, we find that,

$$\langle L^{\mu\nu} \rangle \sim \frac{q^2}{3}\left(-g^{\mu\nu} + \frac{q^\mu q^\nu}{q^2} \right), \tag{A3}$$

with $l_{1,2}$ as the momenta of the two leptons and $q = l_1 + l_2$ as the momentum of the vector boson. In original FEWZ, individual components of $Q_{\mu\nu}$ are not separately available since they only appear in the product of two currents in the matrix element. For the DY-like part of the VH production, it can be thought as a gauge boson V^* first produced via the DY process, and subsequently decaying to V and H, where V further decays to two leptons. Because of gauge invariance, we can write the new squared matrix element for Higgsstrahlung process as,

$$\overline{|\mathcal{M}_{VH}|^2} \sim Q_{\mu\nu} L'^{\mu\nu}, \tag{A4}$$

where $L'^{\mu\nu}$ denotes the square of the new lepton current. If we integrate inclusively over the V and H phase space, the new lepton current becomes,

$$
\begin{aligned}
\langle L'^{\mu\nu} \rangle \;\sim\;& \frac{q'^2}{3}\left(-g^{\mu\nu} + \frac{q'^\mu q'^\nu}{q'^2}\right) \\
\to\;& \frac{q'^2}{3}\left\{-g^{\mu\nu}\left(\frac{2}{3} + \frac{(q\cdot q')^2}{3\,q^2\,q'^2}\right) + \frac{q^\mu q^\nu}{q^2}\left(-\frac{1}{3} + \frac{4}{3}\frac{(q\cdot q')^2}{q^2\,q'^2}\right)\right\},
\end{aligned}
\tag{A5}
$$

in which q' and q are the momenta of V and V^* respectively, and $q\cdot q' = (q^2 + q'^2 - m_H^2)/2$. The second piece drops out when multiplied with the quark current, and therefore we arrive at,

$$
Q_{\mu\nu}\langle L'^{\mu\nu}\rangle = \frac{q'^2}{q^2}Q_{\mu\nu}\langle L^{\mu\nu}\rangle\left(\frac{2}{3} + \frac{(q\cdot q')^2}{3\,q^2\,q'^2}\right).
\tag{A6}
$$

However, Eq. (A6) does not apply to the case where acceptance cut is placed on leptons, the vector boson or the Higgs. We can use

$$
\begin{aligned}
\langle L^{\mu\nu}L^{\rho\sigma}\rangle \;=\;& \frac{q^4}{4}\left\{\frac{2}{5}\left(-g^{\mu\nu} + \frac{q^\mu q^\nu}{q^2}\right)\left(-g^{\rho\sigma} + \frac{q^\rho q^\sigma}{q^2}\right) + \right. \\
& \left. \frac{1}{15}\left[\left(-g^{\mu\rho} + \frac{q^\mu q^\rho}{q^2}\right)\left(-g^{\nu\sigma} + \frac{q^\nu q^\sigma}{q^2}\right) + \left(-g^{\mu\sigma} + \frac{q^\mu q^\sigma}{q^2}\right)\left(-g^{\nu\rho} + \frac{q^\nu q^\rho}{q^2}\right)\right]\right\},
\end{aligned}
\tag{A7}
$$

in combination with Eq. (A3) and obtain

$$
Q_{\mu\nu}L'^{\mu\nu} = 30\,Q_{\mu\nu}\frac{\langle L^{\mu\nu}L^{\rho\sigma}\rangle}{q^4}L'_{\rho\sigma} - 9\,Q_{\mu\nu}\frac{\langle L^{\mu\nu}\rangle}{q^2}\left(-g^{\rho\sigma} + \frac{q^\rho q^\sigma}{q^2}\right)L'_{\rho\sigma}.
\tag{A8}
$$

The average is performed by integrating over the original lepton phase space inclusively, and arbitrary cuts can be applied on the new vector boson and Higgs, as well the final leptonic final states, as long as no asymmetry related observables are measured. It can be seen that Eq. (A6) is easily recovered by substituting the integrated form of $L'_{\rho\sigma}$ into Eq. (A8). Because only the product $Q_{\mu\nu}L^{\mu\nu}$ appears in Eq. (A8), FEWZ can be modified in a relatively straightforward way.

Appendix B: Fixed-order matrix elements

In this appendix, we list all the ingredients needed for a NNLL$'$ resummation for $pp \to VH$ production in 0-jet bin. We start with the fixed order matrix elements to $\mathcal{O}(\alpha_s^2)$

1. Hard Function

The spin and color averaged LO matrix elements squared for processes $q\bar{q} \to ZH \to \bar{l}lH$ and $q\bar{q} \to WH \to \nu l H$ are proportional to that of LO DY processes,

$$\overline{|\mathcal{M}_Z|^2} = \frac{1}{12}(4\pi\alpha)^2 \left(\frac{4(|g^+_{qqZ}g^+_{llZ}|^2 + |g^-_{qqZ}g^-_{llZ}|^2)s_{q\bar{l}}s_{\bar{q}l} + 4(|g^+_{qqZ}g^-_{llZ}|^2 + |g^-_{qqZ}g^+_{llZ}|^2)s_{ql}s_{\bar{q}\bar{l}}}{(s_{l\bar{l}} - M_Z^2)^2 + M_Z^2\Gamma_Z^2} \right),$$

$$\overline{|\mathcal{M}_{W^-}|^2} = \frac{1}{12}\frac{(4\pi\alpha)^2}{s_w^4}\frac{s_{q\bar{\nu}}s_{\bar{q}l}}{(s_{l\bar{\nu}} - M_W^2)^2 + M_W^2\Gamma_W^2},$$

$$\overline{|\mathcal{M}_{W^+}|^2} = \frac{1}{12}\frac{(4\pi\alpha)^2}{s_w^4}\frac{s_{q\bar{l}}s_{\bar{q}\nu}}{(s_{\nu\bar{l}} - M_W^2)^2 + M_W^2\Gamma_W^2}, \tag{B1}$$

with $s_{ij} = 2\,p_i \cdot p_j$, $g^+_{ffZ} = -Q_f s_w/c_w$ and $g^-_{ffZ} = (I^3_{W,f} - Q_f s_w^2)/s_w/c_w$. Therefore

$$\overline{|\mathcal{M}_{ZH}|^2} = \frac{4\pi\alpha M_Z^2}{s_w^2 c_w^2}\frac{1}{(s_{q\bar{q}} - M_Z^2)^2 + M_Z^2\Gamma_Z^2}\overline{|\mathcal{M}_Z|^2},$$

$$\overline{|\mathcal{M}_{W^\pm H}|^2} = \frac{4\pi\alpha M_W^2}{s_w^2}\frac{1}{(s_{q\bar{q}} - M_W^2)^2 + M_W^2\Gamma_W^2}\overline{|\mathcal{M}_{W^\pm}|^2}, \tag{B2}$$

where M_Z and M_W are the masses for Z and W bosons, respectively and Γ_Z and Γ_W are the widths.

The NNLO hard function for Drell-Yan has been known for a while and can be found for instance in [44], which gives

$$H_{q\bar{q}V}(Q^2,\mu) = 1 + \frac{\alpha_s}{4\pi}C_F\left(-2L^2 - 6L - 16 + \frac{7\pi^2}{3}\right)$$

$$+ \left(\frac{\alpha_s}{4\pi}\right)^2\left[2C_F\left(C_F H_F + C_A H_A + T_F n_f H_f\right) + C_F^2 G_F\right], \tag{B3}$$

with

$$H_F = \frac{L^4}{2} + 3L^3 + \left(\frac{25}{2} - \frac{19\pi^2}{6}\right)L^2 + \left(\frac{45}{2} - \frac{15\pi^2}{2} - 24\zeta_3\right)L + \frac{255}{8} - 9\pi^2 + \frac{157\pi^4}{360} - 30\zeta_3,$$

$$H_A = -\frac{11}{9}L^3 - \left(\frac{233}{18} - \frac{\pi^2}{3}\right)L^2 - \left(\frac{2545}{54} - \frac{22\pi^2}{9} - 26\zeta_3\right)L - \frac{51157}{648} + \frac{1061\pi^2}{108} - \frac{4\pi^4}{45} + \frac{313}{9}\zeta_3,$$

$$H_f = \frac{4}{9}L^3 + \frac{38}{9}L^2 + \left(\frac{418}{27} - \frac{8\pi^2}{9}\right)L + \frac{4085}{162} - \frac{91\pi^2}{27} + \frac{4}{9}\zeta_3,$$

$$G_F = L^4 + 6L^3 + \left(25 + \frac{5\pi^2}{3}\right)L^2 + \left(48 + 5\pi^2\right)L + 64 - \frac{29\pi^2}{3} + \frac{49\pi^4}{36}. \tag{B4}$$

Here we have abbreviated $L \equiv \log(\mu^2/Q^2)$.

14

2. Soft Function

The full two-loop soft function can be extracted from Ref. [25] by suitably replacing the color factors, and is found to have the form

$$
\begin{aligned}
S_{q\bar{q}}(p_T^{veto}, R, \mu, \nu) &= 1 + \frac{\alpha_s(\mu)}{4\pi} C_F \left[2\Gamma_0 L_S^\mu (L_S^\mu - 2L_S^\nu) - \frac{\pi^2}{3} \right] \\
&+ \frac{\alpha_s^2(\mu)}{(4\pi)^2} \left\{ \frac{1}{2} C_F^2 \left[2\Gamma_0 L_S^\mu (L_S^\mu - 2L_S^\nu) - \frac{\pi^2}{3} \right]^2 + 2\beta_0 C_F L_S^\mu \left[2\Gamma_0 L_S^\mu \left(\frac{1}{3} L_S^\mu - L_S^\nu \right) - \frac{\pi^2}{3} \right] \right. \\
&+ \left. 2\Gamma_1 C_F L_S^\mu (L_S^\mu - 2L_S^\nu) + \gamma_{S1}^q L_S^\mu + \gamma_{\nu1}^q(R) L_S^\nu + s_2(R) \right\},
\end{aligned} \tag{B5}
$$

with $L_S^\mu \equiv \log \frac{\mu}{p_T^{veto}}$, and $L_S^\nu \equiv \log \frac{\nu}{p_T^{veto}}$.

The dependence on the jet algorithm starts to enter at two loops through the two-loop ν anomalous dimension, $\gamma_{\nu1}^g(R)$, which determines the coefficient of the single logarithm of $\ln(\nu/p_T^{veto})$, as well as the non-logarithmic two-loop soft constant, $s_2(R)$. For the coefficients of the soft non-cusp anomalous dimensions we find

$$
\begin{aligned}
\gamma_{S0}^q &= 0, \\
\gamma_{S1}^q &= 8C_F \left[\left(\frac{52}{9} - 4(1+\pi^2)\ln 2 + 11\zeta_3 \right) C_A + \left(\frac{2}{9} + \frac{7\pi^2}{12} - \frac{20}{3}\ln 2 \right) \beta_0 \right], \\
\gamma_{\nu0}^q(R) &= 0, \\
\gamma_{\nu1}^q(R) &= -16C_F \left[\left(\frac{17}{9} - (1+\pi^2)\ln 2 + \zeta_3 \right) C_A + \left(\frac{4}{9} + \frac{\pi^2}{12} - \frac{5}{3}\ln 2 \right) \beta_0 \right] + C_2(R). \tag{B6}
\end{aligned}
$$

Here, $C_2(R)$ is the clustering correction due to the jet algorithm:

$$
\begin{aligned}
C_2(R) &= 2C_F \left[\left(1 - \frac{8\pi^2}{3} \right) C_A + \left(\frac{23}{3} - 8\ln 2 \right) \beta_0 \right] \ln R^2 \\
&+ 15.62 C_F C_A - 9.17 C_F \beta_0, \tag{B7}
\end{aligned}
$$

up to $\mathcal{O}(R^2)$ corrections whose explicit form can be lifted from Ref. [24].

The two-loop soft function constant $s_2(R)$, which is not determined from RGE constraints, is

$$
\begin{aligned}
s_2(R) &= C_F \left[\left(\frac{19}{3} - 10\ln 2 + 8\zeta_3 \right) C_A + \left(-\frac{163}{9} + \frac{58}{3}\ln 2 + 8\ln^2 2 \right) \beta_0 \right] \ln R^2 \\
&- 18.68 C_F C_A - 3.25 C_F \beta_0 + s_2^{R_{\text{sub}}}(R), \tag{B8}
\end{aligned}
$$

where $s_2^{R_{\text{sub}}}(R) \sim R^2$.

3. Beam Function

When matching onto pdfs, the NNLO beam function has the form

$$B_q(x, \mu_B, \nu_B) = \sum_j \int_x^1 \frac{\mathrm{d}z}{z} \, \mathcal{I}_{qj}(R, z, \mu_B, \nu_B) \, f_j\left(\frac{x}{z}, \mu_B\right) , \tag{B9}$$

where the matching kernels $\mathcal{I}_{qj}$ read

$$\mathcal{I}_{qj} = \delta(1 - z)\delta_{qj} + \frac{\alpha_s}{4\pi}\mathcal{I}_{qj}^{(1)} + \left(\frac{\alpha_s}{4\pi}\right)^2 \mathcal{I}_{qj}^{(2)} , \tag{B10}$$

with

$$\mathcal{I}_{q_i q_i}^{(1)} = 2C_F \left(4 L_\mu L_\nu \delta(1 - z) - 2L_\mu p_{q_i q_i}^{(0)}(z) + I_{q_i q_i}^{(1)}(z)\right) ,$$
$$\mathcal{I}_{qg}^{(1)} = 2T_F \left(-2L_\mu p_{qg}^{(0)}(z) + I_{qg}^{(1)}(z)\right) , \tag{B11}$$

given that $L_\mu \equiv \log \frac{\mu}{p_T^{veto}}$ and $L_\nu \equiv \log \frac{\nu}{Q}$.

The form of the two-loop matching coefficient $\mathcal{I}^{(2)}$ can be obtained by expanding the NNLL$'$ resummed beam function and matching onto PDFs, which results in

$$
\begin{aligned}
\mathcal{I}_{q_i q_i}^{(2)}(z) = {} & L_\mu^2 L_\nu^2 \, 2\Gamma_0^2 C_F^2 \, \delta(1 - z) + L_\mu^2 L_\nu \left(2\Gamma_0 C_F \beta_0 \delta(1 - z) - 8C_F^2 \Gamma_0 \, p_{q_i q_i}^{(0)}(z)\right) \\
& + \; L_\mu L_\nu \left(4\Gamma_0 C_F^2 I_{q_i q_i}^{(1)}(z) + 2\Gamma_1 C_F \, \delta(1 - z)\right) \\
& + \; L_\mu^2 \left(-4C_F \beta_0 p_{q_i q_i}^{(0)}(z) + 8C_F^2 \, p_{q_i q_i}^{(0)} \otimes p_{q_i q_i}^{(0)}(z) + 8C_F T_F \, p_{q_i g}^{(0)} \otimes p_{g q_i}^{(0)}(z)\right) \\
& + \; L_\mu \left\{4C_F \beta_0 I_{q_i q_i}^{(1)}(z) + \gamma_{B,1}^q \delta(1 - z) - 8\bar{p}_{q_i q_i}^{(1)}(z) - 8C_F^2 \, I_{q_i q_i}^{(1)} \otimes p_{q_i q_i}^{(0)} - 8C_F T_F \, I_{q_i g}^{(1)} \otimes p_{g q_i}^{(0)}\right\} \\
& + \; L_\nu \left(-\frac{1}{2}\gamma_{\nu,1}^q \delta(1 - z)\right) + I_{q_i q_i}^{(2)}(R, z) ,
\end{aligned} \tag{B12}
$$

$$
\begin{aligned}
\mathcal{I}_{q_i g}^{(2)}(z) = {} & L_\mu^2 L_\nu \left(-8\Gamma_0 C_F T_F \, p_{q_i g}^{(0)}(z)\right) + L_\mu L_\nu \left(4\Gamma_0 C_F T_F \, I_{q_i g}^{(1)}(z)\right) \\
& + \; L_\mu^2 \left\{-\left(4\beta_0 + 2\gamma_{B,0}^q\right) T_F \, p_{q_i g}^{(0)}(z) + 8C_F T_F \, p_{q_i q_i}^{(0)} \otimes p_{q_i g}^{(0)}(z) + 8C_A T_F \, p_{q_i g}^{(0)} \otimes \bar{p}_{gg}^{(0)}(z)\right\} \\
& + \; L_\mu \left\{(4\beta_0 + 2\gamma_{B,0}^q) T_F \, I_{q_i g}^{(1)}(z) - 8p_{q_i g}^{(1)}(z) - 8C_F T_F \, I_{q_i q_i}^{(1)} \otimes p_{q_i g}^{(0)}(z) - 8C_A T_F \, I_{q_i g}^{(1)} \otimes \bar{p}_{gg}^{(0)}(z)\right\} \\
& + \; I_{q_i g}^{(2)}(R, z) ,
\end{aligned} \tag{B13}
$$

and

$$
\begin{aligned}
\mathcal{I}_{q_i q_j}^{(2)}(z) = {} & L_\mu^2 \left(8C_F T_F \, p_{q_i g}^{(0)} \otimes p_{g q_j}^{(0)}(z)\right) + L_\mu \left(-8p_{q_i q_j}^{(1)}(z) - 8C_F T_F \, I_{q_i g}^{(1)} \otimes p_{g q_j}^{(0)}(z)\right) \\
& + I_{q_i q_j}^{(2)}(R, z) ,
\end{aligned} \tag{B14}
$$

where $\bar{p}_{kj}^{(i)}(z)$ is the i-th order full splitting function including properly the $\delta_{kj}\delta(1 - z)$ while $p_{kj}^{(i)}(z)$ does not. In both cases, an overall color factor has been extracted from the splitting

16

kernel. In Eq. (B14), q_j in the subscript stands for either quarks with different flavors from q_i or any possible anti-quarks.

The non-logarithmic terms $I_{ij}^{(2)}(R, z)$ can not be determined by the expansion and have to be computed explicitly, and are not yet known. However, for small R, the dominant $\log R$ piece can be calculated in a very simple way, as explained in the text, which leads to

$$
\begin{aligned}
I_{q_i q_i, \log R}^{(2)} &= \frac{2}{9} C_F \left(\left(-12\pi^2 + 131 - 132 \log(2) \right) C_A + (24 \log(2) - 23) n_f T_F \right) \log(R^2) \, p_{q_i q_i}^{(0)}(z) \, , \\
I_{q_i g, \log R}^{(2)} &= 4 C_F T_F \left(-\frac{\pi^2}{3} + 3 - 3 \log(2) \right) \log(R^2) p_{q_i, g}^{(0)}(z) \, .
\end{aligned}
\tag{B15}
$$

The contribution from the remaining piece can be obtained by fitting with the fixed order NNLO QCD calculation.

Appendix C: RG running

All the functions in the previous section have to be evolved from their natural scales to a common scale μ to evaluate the cross section. Other than the conventional RG evolution,

$$
\mu \frac{\mathrm{d}F}{\mathrm{d}\mu} = \Gamma_F^\mu(\mu) F(\mu) \, ,
\tag{C1}
$$

due to the existence of the rapidity divergence in SCET resulted from the multipole expansion, another rapidity evolution

$$
\nu \frac{\mathrm{d}F_{B,S}}{\mathrm{d}\nu} = \Gamma_{B,S}^\nu(\nu) F_{B,S}(\nu) \, ,
\tag{C2}
$$

for the soft and the beam functions is needed to resum a series of large rapidity logs. The general solution to these RG equations can be formally written as

$$
F(\mu, \nu) = U(\mu, \nu; \mu_0, \nu_0) F(\mu_0, \nu_0) \, ,
\tag{C3}
$$

where the natural scales (μ_0, ν_0) for each function are determined by demanding that no large logs exist in the fixed order matrix elements. The evolution of the hard Wilson coefficient $C_H^{q\bar{q}V}$ which is related to the hard function by $H = CC^\dagger$, is given by

$$
U_{C_H}(\mu, \mu_H) = \exp \left(2 C_F S(\mu, \mu_H) - C_F A_\Gamma \log \frac{-Q^2 - i0^+}{\mu_H^2} - A_H(\mu, \mu_H) \right) \, ,
\tag{C4}
$$

where a natural choice of μ_H will be $\mu_H^2 = -Q^2 - i0^+$ to stabilize the fixed order expansion of the hard function. By doing so, a towers of π^2 terms will also be resummed. Therefore

17

the evolution of the hard function is given by

$$
U_H = U_H^{\log} \times \exp\left(2\Re e\left[2C_F S(\mu_H, -\mu_H) - C_F A_\Gamma(\mu_H, -\mu_H)\log\frac{Q^2}{\mu_H^2} - A_H(\mu_H, -\mu_H)\right]\right)
$$

$$
= U_H^{\log}(\mu, \mu_H)\exp\left(\frac{\pi\alpha_s(\mu_H)C_F}{2}\left[1 + \frac{1}{4\pi}\left(\frac{\Gamma_1}{\Gamma_0} - \frac{\gamma_H^0}{\Gamma_0}\frac{\beta_0}{C_F} - \beta_0\log\frac{Q^2}{\mu_H^2}\right)\alpha_s(\mu_H)\right]\right) \quad \text{(C5)}
$$

Here $U_H^{\log} = U_C U_C^\dagger$ is the normal evolution for the global log resummation.

The running of the beam function is found to be

$$
U_{B,a}(\mu, \nu; \mu_B, \nu_B) = \exp\left(-C_F A_\Gamma\left(\mu, p_T^{veto}\right)\log\frac{\nu^2}{\nu_B^2}\right)\exp\left(-C_F A_\Gamma(\mu, \mu_B)\log\frac{\nu_B^2}{\omega_a^2} - A_{B_a}(\mu, \mu_B)\right),
$$

$$
\times \exp\left(-\frac{1}{2}\gamma_\nu^q\left[\alpha_s(p_T^{veto}), R\right]\log\frac{\nu}{\nu_B}\right). \quad \text{(C6)}
$$

The central value of (μ_B, ν_B) will be chosen as (p_T^{veto}, ω_a).

For the soft function, we have

$$
U_S(\mu, \nu; \mu_S, \nu_B) = \exp\left(2C_F A_\Gamma(\mu, p_T^{veto})\log\frac{\nu^2}{\nu_S^2}\right)\exp\left(-4C_F S(\mu, \mu_S) - A_S(\mu, \mu_S)\right)
$$

$$
\times \exp\left(2C_F A_\Gamma(\mu, \mu_S)\log\frac{\nu_S^2}{\mu_S^2}\right)\exp\left(\gamma_\nu^q\left[\alpha_s(p_T^{veto}), R\right]\log\frac{\nu}{\nu_S}\right). \quad \text{(C7)}
$$

The natural scale (μ_S, ν_S) for the soft sector is (p_T^{veto}, p_T^{veto}).

In the equations above, the expansion of these quantities in α_s up to terms needed for NNLL resummation are given by

$$
S(\mu_f, \mu_i) = \frac{\Gamma_0}{4\beta_0^2}\left\{\frac{4\pi}{\alpha_s(\mu_i)}\left(1 - \frac{1}{r} - \ln r\right) + \left(\frac{\Gamma_1}{\Gamma_0} - \frac{\beta_1}{\beta_0}\right)(1 - r + \ln r) + \frac{\beta_1}{2\beta_0}\ln^2 r\right.
$$

$$
+ \frac{\alpha_s(\mu_i)}{4\pi}\left[\left(\frac{\beta_1\Gamma_1}{\beta_0\Gamma_0} - \frac{\beta_2}{\beta_0}\right)(1 - r + r\ln r) + \left(\frac{\beta_1^2}{\beta_0^2} - \frac{\beta_2}{\beta_0}\right)(1 - r)\ln r\right.
$$

$$
\left.\left. - \left(\frac{\beta_1^2}{\beta_0^2} - \frac{\beta_2}{\beta_0} - \frac{\beta_1\Gamma_1}{\beta_0\Gamma_0} + \frac{\Gamma_2}{\Gamma_0}\right)\frac{(1 - r)^2}{2}\right]\right\}, \quad \text{(C8)}
$$

with $r = \alpha_s(\mu_f)/\alpha_s(\mu_i)$, and

$$
A_\Gamma(\mu_f, \mu_i) = \frac{\Gamma_0}{2\beta_0}\left\{\log r + \frac{\alpha_s(\mu_i)}{4\pi}\left(\frac{\Gamma_1}{\Gamma_0} - \frac{\beta_1}{\beta_0}\right)(r - 1)\right.
$$

$$
\left. + \frac{\alpha_s^2(\mu_i)}{16\pi^2}\left[\frac{\Gamma_2}{\Gamma_0} - \frac{\beta_2}{\beta_0} - \frac{\beta_1}{\beta_0}\left(\frac{\Gamma_1}{\Gamma_0} - \frac{\beta_1}{\beta_0}\right)\right]\frac{r^2 - 1}{2}\right\}. \quad \text{(C9)}
$$

Also A_H, A_B and A_S are needed to the α_s order, which can be obtained by substituting the Γ_0 and Γ_1 in A_Γ with $\gamma_{i,0}$ and $\gamma_{i,1}$ for each function and truncating out the α_s^2 terms.

18

Appendix D: Input ingredients

Here we group all the parameters and equations including splitting functions and convolutions which are used in NNLL$'$ resummation

The 0-th order modified splitting kernels needed in the beam function are

$$
\begin{aligned}
p_{gg}^{(0)}(z) &= \frac{2z}{(1-z)_+} + 2z(1-z) + 2\frac{1-z}{z}\,, \\
p_{qq}^{(0)}(z) &= \frac{1+z^2}{(1-z)_+}\,, \\
p_{gq}^{(0)}(z) &= \frac{1+(1-z)^2}{z}\,, \\
p_{qg}^{(0)}(z) &= 1 - 2z + 2z^2\,,
\end{aligned}
\tag{D1}
$$

and

$$
\begin{aligned}
\bar{p}_{q_i q_j}^{(0)}(z) &= \frac{3}{2}\delta_{ij}\delta(1-z) + p_{qq}^{(0)}(z)\,, \\
\bar{p}_{gg}^{(0)}(z) &= \frac{\beta_0}{2C_A}\delta(1-z) + p_{gg}^{(0)}(z)\,.
\end{aligned}
\tag{D2}
$$

The 1-th order splitting functions give [45]

$$
\begin{aligned}
p_{q_i q_j}^{(1)} &= \delta_{ij}p_{qq}^{V,(1)} + p_{qq}^{S,(1)}\,, \\
p_{q_i \bar{q}_j}^{(1)} &= \delta_{ij}p_{q\bar{q}}^{V,(1)} + p_{q\bar{q}}^{S,(1)}\,,
\end{aligned}
\tag{D3}
$$

and

$$
\begin{aligned}
p_{qq}^{V,(1)} &= C_F^2\Big\{ -\big[2\ln x\ln(1-x) + \frac{3}{2}\ln x\big]p_{qq}^{(0)}(x) \\
&\quad -\Big(\frac{3}{2} + \frac{7}{2}x\Big)\ln x - \frac{1}{2}(1+x)\ln^2 x - 5(1-x)\Big\} \\
&\quad +C_F C_A\Big\{ \Big[\frac{1}{2}\ln^2 x + \frac{11}{6}\ln x + \frac{67}{18} - \frac{\pi^2}{6}\Big]p_{qq}^{(0)}(x) + (1+x)\ln x + \frac{20}{3}(1-x)\Big\} \\
&\quad +n_f C_F T_F\Big\{ -\Big[\frac{2}{3}\ln x + \frac{10}{9}\Big]p_{qq}^{(0)}(x) - \frac{4}{3}(1-x))\Big\}\,, \\
p_{q\bar{q}}^{V,(1)} &= C_F\Big(C_F - \frac{C_A}{2}\Big)\Big\{2p_{qq}^{(0)}(-x)S_2(x) + 2(1+x)\ln x + 4(1-x)\Big\}\,,
\end{aligned}
\tag{D4}
$$

$$
\begin{aligned}
p_{qq}^{S,(1)} &= p_{q\bar{q}}^{S,(1)} \\
&= C_F T_F\Big\{\frac{20}{9x} - 2 + 6x - \frac{56}{9}x^2 + \Big(1 + 5x + \frac{8}{3}x^2\Big)\ln x - (1+x)\ln^2 x\Big\}\,,
\end{aligned}
\tag{D5}
$$

19

$$p_{qg}^{(1)} = \frac{C_F T_F}{2}\left\{4 - 9x - (1 - 4x)\ln x - (1 - 2x)\ln^2 x + 4\ln(1 - x)\right.$$
$$+ \left[2\ln^2\left(\frac{1 - x}{x}\right) - 4\ln\left(\frac{1 - x}{x}\right) - \frac{2}{3}\pi^2 + 10\right]p_{qg}^{(0)}(x)\left.\right\}$$
$$+ \frac{C_A T_F}{2}\left\{\frac{182}{9} + \frac{14}{9}x + \frac{40}{9x} + \left(\frac{136}{3}x - \frac{38}{3}\right)\ln x - 4\ln(1 - x) - (2 + 8x)\ln^2 x\right.$$
$$+ \left[-\ln^2 x + \frac{44}{3}\ln x - 2\ln^2(1 - x) + 4\ln(1 - x) + \frac{\pi^2}{3} - \frac{218}{9}\right]p_{qg}^{(0)}(x)$$
$$+ 2p_{qg}^{(0)}(-x)S_2(x)\left.\right\}, \tag{D6}$$

where the function $S_2(x)$ is defined as

$$S_2(x) = \int_{\frac{x}{1+x}}^{\frac{1}{1+x}}\frac{dz}{z}\ln\left(\frac{1 - z}{z}\right) = \frac{\ln^2 x}{2} - \ln x \ln(1 + x) + \text{Li}_2\left(\frac{x}{1 + x}\right) - \text{Li}_2\left(\frac{1}{1 + x}\right)$$
$$= \frac{\ln^2 x}{2} - \frac{\pi^2}{6} - 2\ln x \ln(1 + x) - 2\,\text{Li}_2(-x). \tag{D7}$$

To extend to the limit $x = 1$, we need to make the substitution

$$\frac{1}{1 - x} \to \frac{1}{[1 - x]_+}. \tag{D8}$$

and add the end-point contributions:

$$\bar{p}_{q_i q_i}^{(1)}(x) = p_{q_i q_i}^{(1)}(x) + \left[C_F^2\left\{\frac{3}{8} - \frac{\pi^2}{2} + 6\zeta_3\right\} + C_F C_A\left\{\frac{17}{24} + \frac{11\pi^2}{18} - 3\zeta_3\right\}\right.$$
$$\left. - n_f C_F T_F\left\{\frac{1}{6} + \frac{2\pi^2}{9}\right\}\right]\delta(1 - x). \tag{D9}$$

The convolutions needed for evaluating the two-loop beam function are

$$p_{qq}^{(0)} \otimes p_{qq}^{(0)}(z) = -2(1-z) + 3(1+z)\log(z) - 4(1+z)\log(1-z)$$
$$+ 8\left(\frac{\log(1-z)}{1-z}\right)_+ - \frac{2\pi^2}{3}\delta(1-z) - 4\frac{\log(z)}{1-z},$$

$$p_{qg}^{(0)} \otimes p_{gq}^{(0)}(z) = -\frac{4z^2}{3} - z + \frac{4}{3z} + 2(z+1)\log(z) + 1,$$

$$p_{qq}^{(0)} \otimes p_{qg}^{(0)}(z) = -3z^2 + \left(-4z^2 + 2z - 1\right)\log(z) + 5z - 2 + 2p_{qg}^{(0)}(z)\log(1-z),$$

$$p_{qg}^{(0)} \otimes \bar{p}_{gg}^{(0)}(z) = -\frac{31z^2}{3} + 8z + \frac{4}{3z} + (8z+2)\log(z) + 2p_{qg}^{(0)}(z)\log(1-z) + 1 + \frac{\beta_0}{2C_A}p_{qg}^{(0)}(z),$$

$$I_{qq}^{(1)} \otimes p_{qq}^{(0)}(z) = -(1-z)(\log(z)+2) + 2I_{qq}^{(1)}(z)\log(1-z),$$

$$I_{qg}^{(1)} \otimes p_{gq}^{(0)}(z) = \frac{2}{3}\left(2z^2 + \frac{1}{z} - 3z\log(z) - 3\right),$$

$$I_{qg}^{(1)} \otimes \bar{p}_{gg}^{(0)}(z) = \frac{2}{3}\left(17z^2 - 15z + \frac{1}{z} - 12z\log(z) - 3\right) + 2I_{qg}^{(1)}(z)\log(1-z) + \frac{\beta_0}{2C_A}I_{qg}^{(1)}(z),$$

$$I_{qq}^{(1)} \otimes p_{qg}^{(0)}(z) = z^2 + z - (2z+1)\log(z) - 2, \tag{D10}$$

with

$$I_{qq}^{(1)}(z) = (1-z), \quad I_{qg}^{(1)}(z) = 2z(1-z). \tag{D11}$$

The parameters going into the anomalous dimensions are listed below. We have

$$\beta_0 = \frac{11}{3}C_A - \frac{4}{3}T_F n_f,$$

$$\beta_1 = \frac{34}{3}C_A^2 - \frac{20}{3}C_A T_F n_f - 4C_F T_F n_f,$$

$$\beta_2 = \frac{2857}{54}C_A^3 + \left(C_F^2 - \frac{205}{18}C_F C_A - \frac{1415}{54}C_A^2\right)2T_F n_f + \left(\frac{11}{9}C_F + \frac{79}{54}C_A\right)4T_F^2 n_f^2,$$

$$\Gamma_0 = 4,$$

$$\Gamma_1 = 4\left[C_A\left(\frac{67}{9} - \frac{\pi^2}{3}\right) - \frac{20}{9}T_F n_f\right],$$

$$\Gamma_2 = 4\left[\left(\frac{245}{6} - \frac{134\pi^2}{27} + \frac{11\pi^4}{45} + \frac{22\zeta_3}{3}\right)C_A^2 + \left(-\frac{418}{27} + \frac{40\pi^2}{27} - \frac{56\zeta_3}{3}\right)C_A T_F n_f$$
$$+ \left(-\frac{55}{3} + 16\zeta_3\right)C_F T_F n_f - \frac{16}{27}T_F^2 n_f^2\right], \tag{D12}$$

for the $\beta[\alpha_s]$ function and cusp anomalous dimensions. And for the non-cusp ones of the

hard Wilson coefficient, we have

$$\gamma_{H0}^q = -6C_F \,,$$

$$\gamma_{H1}^q = C_F^2(-3 + 4\pi^2 - 48\zeta_3) + C_F C_A \left(-\frac{961}{27} - \frac{11\pi^2}{3} + 52\zeta_3 \right)$$

$$+ n_f C_F T_F \left(\frac{260}{27} + \frac{4\pi^2}{3} \right) . \tag{D13}$$

The soft non-cusp anomalous dimensions could be found in the previous sections, and the anomalous dimension for the beam function can be obtained through the consistency condition $\gamma_B^\mu = -\gamma_H^\mu - \frac{1}{2}\gamma_S^\mu$ and $\gamma_B^\nu = -\frac{1}{2}\gamma_S^\nu$ for the normal RG and the SCET rapidity evolution, respectively.

Here the $\beta[\alpha_s]$ function is expanded as,

$$\beta[\alpha_s] = -2\alpha_s \sum_{n=0} \beta_n \left(\frac{\alpha_s}{4\pi} \right)^{n+1} , \tag{D14}$$

and the rest of the quantities are expanded as

$$F[\alpha_s] = \frac{\alpha_s}{4\pi} F_0 + \left(\frac{\alpha_s}{4\pi} \right)^2 F_1 + \cdots . \tag{D15}$$

Note that we can use

$$\mathrm{d}\log\mu = \frac{1}{\beta[\alpha_s]} \mathrm{d}\alpha_s \tag{D16}$$

to convert the $\log\mu$ integration to α_s integration.

As for the expansion of NNLL$'$ resummation, we need to use

$$\frac{1}{\alpha_s(\mu_i)} = \frac{X}{\alpha_s(\mu)} + \frac{\beta_1}{4\pi\beta_0} \log(X) + \frac{\alpha_s(\mu)}{16\pi^2} \left[\frac{\beta_2}{\beta_0} \left(1 - \frac{1}{X} \right) + \frac{\beta_1^2}{\beta_0^2} \left(\frac{\log(X)}{X} + \frac{1}{X} - 1 \right) \right] \tag{D17}$$

with

$$X = 1 - \frac{\alpha_s(\mu)}{4\pi} \beta_0 \log \frac{\mu^2}{\mu_i^2} . \tag{D18}$$

For $\mu_i = -\mu - i0^+$, we have

$$X = 1 - ia(\mu) \,, \tag{D19}$$

with $a(\mu) \equiv \alpha_s(\mu)\beta_0/4$ treated as an $\mathcal{O}(\alpha_s)$ parameter.

---

[1] G. Aad *et al.* [ATLAS Collaboration], Phys. Lett. B **716**, 1 (2012) [arXiv:1207.7214 [hep-ex]].

[2] S. Chatrchyan *et al.* [CMS Collaboration], Phys. Lett. B **716**, 30 (2012) [arXiv:1207.7235 [hep-ex]].

[3] J. M. Butterworth, A. R. Davison, M. Rubin and G. P. Salam, Phys. Rev. Lett. **100**, 242001 (2008) [arXiv:0802.2470 [hep-ph]].

[4] The ATLAS collaboration, ATLAS-CONF-2013-079.

[5] G. Aad *et al.* [ATLAS Collaboration], Phys. Lett. B **718**, 369 (2012) [arXiv:1207.0210 [hep-ex]].

[6] S. Chatrchyan *et al.* [CMS Collaboration], arXiv:1310.3687 [hep-ex].

[7] S. Chatrchyan *et al.* [CMS Collaboration], Phys. Lett. B **710**, 284 (2012) [arXiv:1202.4195 [hep-ex]].

[8] [ATLAS Collaboration], ATLAS-CONF-2013-011.

[9] CMS Collaboration [CMS Collaboration], CMS-PAS-HIG-13-018.

[10] T. Han and S. Willenbrock, Phys. Lett. B **273**, 167 (1991).

[11] R. Hamberg, W. L. van Neerven and T. Matsuura, Nucl. Phys. B **359**, 343 (1991) [Erratum-ibid. B **644**, 403 (2002)].

[12] R. V. Harlander and W. B. Kilgore, Phys. Rev. Lett. **88**, 201801 (2002) [hep-ph/0201206].

[13] G. Ferrera, M. Grazzini and F. Tramontano, Phys. Rev. Lett. **107**, 152003 (2011) [arXiv:1107.1164 [hep-ph]].

[14] S. Dawson, T. Han, W. K. Lai, A. K. Leibovich and I. Lewis, Phys. Rev. D **86**, 074007 (2012) [arXiv:1207.4207 [hep-ph]].

[15] D. Y. Shao, C. S. Li and H. T. Li, arXiv:1309.5015 [hep-ph].

[16] A. Banfi, G. P. Salam and G. Zanderighi, JHEP **1206**, 159 (2012) [arXiv:1203.5773 [hep-ph]].

[17] A. Banfi, P. F. Monni, G. P. Salam and G. Zanderighi, Phys. Rev. Lett. **109**, 202001 (2012) [arXiv:1206.4998 [hep-ph]].

[18] C. W. Bauer, S. Fleming and M. E. Luke, Phys. Rev. D **63**, 014006 (2000) [hep-ph/0005275].

[19] C. W. Bauer, S. Fleming, D. Pirjol, and I. W. Stewart, Phys. Rev. **D63**, 114020 (2001), hep-ph/0011336.

[20] C. W. Bauer and I. W. Stewart, Phys. Lett. B **516**, 134 (2001) [hep-ph/0107001].

[21] C. W. Bauer, D. Pirjol, and I. W. Stewart, Phys. Rev. **D65**, 054022 (2002), hep-ph/0109045.

[22] C. W. Bauer, S. Fleming, D. Pirjol, I. Z. Rothstein, and I. W. Stewart, Phys. Rev. **D66**, 014017 (2002), hep-ph/0202088.

[23] T. Becher and M. Neubert, JHEP **1207**, 108 (2012) [arXiv:1205.3806 [hep-ph]].

[24] T. Becher, M. Neubert and L. Rothen, arXiv:1307.0025 [hep-ph].

[25] I. W. Stewart, F. J. Tackmann, J. R. Walsh and S. Zuberi, arXiv:1307.1808 [hep-ph].

[26] X. Liu and F. Petriello, Phys. Rev. D **87**, 014018 (2013) [arXiv:1210.1906 [hep-ph]].

[27] X. Liu and F. Petriello, Phys. Rev. D **87**, 094027 (2013) [arXiv:1303.4405 [hep-ph]].

[28] R. Boughezal, X. Liu, F. Petriello, F. J. Tackmann and J. R. Walsh, arXiv:1312.4535 [hep-ph].

[29] S. Alioli and J. R. Walsh, arXiv:1311.5234 [hep-ph].

[30] R. Gavin, Y. Li, F. Petriello and S. Quackenbush, Comput. Phys. Commun. **182**, 2388 (2011) [arXiv:1011.3540 [hep-ph]].

[31] R. Gavin, Y. Li, F. Petriello and S. Quackenbush, Comput. Phys. Commun. **184**, 208 (2013) [arXiv:1201.5896 [hep-ph]].

[32] Y. Li and F. Petriello, Phys. Rev. D **86**, 094034 (2012) [arXiv:1208.5967 [hep-ph]].

[33] O. Brein, R. V. Harlander and T. J. E. Zirke, Comput. Phys. Commun. **184**, 998 (2013)

[arXiv:1210.5347 [hep-ph]].

[34] J. M. Campbell and R. K. Ellis, Nucl. Phys. Proc. Suppl. **205-206**, 10 (2010) [arXiv:1007.3492 [hep-ph]].

[35] T. Gleisberg, S. Hoeche, F. Krauss, A. Schalicke, S. Schumann and J. -C. Winter, JHEP **0402**, 056 (2004) [hep-ph/0311263].

[36] J. M. Campbell, K. Hatakeyama, J. Huston, F. Petriello, J. Andersen, L. Barze, H. Beauchemin and T. Becher *et al.*, arXiv:1310.5189 [hep-ph].

[37] SHeinemeyer *et al.* [LHC Higgs Cross Section Working Group Collaboration], arXiv:1307.1347 [hep-ph].

[38] J. -y. Chiu, A. Jain, D. Neill and I. Z. Rothstein, Phys. Rev. Lett. **108**, 151601 (2012) [arXiv:1104.0881 [hep-ph]].

[39] J. -Y. Chiu, A. Jain, D. Neill and I. Z. Rothstein, JHEP **1205**, 084 (2012) [arXiv:1202.0814 [hep-ph]].

[40] V. Ahrens, T. Becher, M. Neubert and L. L. Yang, Phys. Rev. D **79**, 033013 (2009) [arXiv:0808.3008 [hep-ph]].

[41] A. D. Martin, W. J. Stirling, R. S. Thorne and G. Watt, Eur. Phys. J. C **63**, 189 (2009) [arXiv:0901.0002 [hep-ph]].

[42] I. W. Stewart and F. J. Tackmann, Phys. Rev. D **85**, 034011 (2012) [arXiv:1107.2117 [hep-ph]].

[43] R. Boughezal, F. Caola, K. Melnikov, F. Petriello and M. Schulze, JHEP **1306**, 072 (2013) [arXiv:1302.6216 [hep-ph]].

[44] T. Becher, M. Neubert and G. Xu, JHEP **0807**, 030 (2008) [arXiv:0710.0680 [hep-ph]].

[45] R. K. Ellis and W. Vogelsang, hep-ph/9602356.